ANALYSIS OF THE PERFORMANCE OF MORPHOLOGICAL EDGE DETECTORS WITH RESPECT TO EDGE ORIENTATION AND DISPLACEMENT

Nelson D.A. Mascarenhas
Ministério de Ciência e Tecnologia
Instituto de Pesquisas Espaciais
Caixa Postal 515 - 12201 - São José dos Campos - SP

Erivaldo A. Silva
UNESP - F.C.T.
Departamento de Cartografia
Presidente Prudente- SP

ABSTRACT

Mathematical Morphology theory has been recently used as a basis for the proposal of new edge detectors in digital images. The purpose of this paper is to present an evaluation of the performance of six morphological edge detectors with respect to sensitivity of their response to edge orientation and edge displacement, in both horizontal and diagonal directions. One example of the application of one of these detectors for the delineation of linear features in urban areas of a Landsat image is also presented.

KEY WORDS: Image Processing, Edge Detection, Mathematical Morphology, Linear Features.

1. EDGE DETECTION AND MATHEMATICAL MORPHOLOGY

Many techniques have been proposed in the literature for the detection of edges in digital images (1). This task provides a basis for a large variety of subsequent phases in the analysis of an image. Recently, mathematical morphology theory has been proposed as a tool to extract edges in images (2). This theory began in the sixties at the École Superieure des Mines de Paris, at Fontainebleau, through G. Matheron (3), J. Serra (4) and their collaborators.

The objective of this work is to evaluate the performance of morphological edge detectors proposed by Lee et al (2), according to the methodology developed by Abdou and Pratt (5) for conventional edge detectors based on enhancement and thresholding. The response of six morphological detectors as a function of edge orientation and edge displacement, in both horizontal and diagonal direction will be studied. Furthermore, an example of application of one of these detectors on an urban Landsat image will be presented.

2. BASIC OPERATIONS OF MATHEMATICAL MORPHOLOGY

The operations of mathematical morphology are performed on an original image to be analysed with a structuring element, with some analogy to the mask that performs the 2-D convolutions. In the case of binary images, let A be the set of points that represent the unitary pixels of the image and B the set of unitary pixels that represent the structuring element.

The dilation of A by B, denoted by A $\oplus$ B, is defined by

$$A \oplus B = \{c/c = a + b \text{ for some } a \in A \text{ e } b \in B\} \qquad (1)$$

Geometrically, dilation is interpreted as the set of points such that the reflection of the structuring element with respect to the origin touches the original set.

The erosion of A by B, denoted by A $\ominus$ B, is defined by

$$A \ominus B = \{ x/x + b \in A \text{ for any } b \in B \} \tag{2}$$

Geometrically, erosion is interpreted as the set of points such that the structuring element which is centered on these points is completely contained in the original set.

In the case of gray level images, dilation and erosion use local maxima and minima of the image, respectively. Accordingly, dilation of a gray level image f by a structuring element b is denoted by d and is defined by (2):

$$d(r,c) = \max_{(i,j)} (f(r-i,c-j) + b(i,j)) \tag{3}$$

where the maximum is taken over all (i,j) over the domain of b such that (r-i, c-j) is over the domain of f. The domain of dilation is the dilation of the domain of f by the domain of b.

Erosion of a gray level image f by a structuring element b is denoted by e and is defined by (2):

$$e(r,c) = \min_{(i,j)} (f(r+i,c+j) - b(i,j)) \tag{4}$$

where the minimum is taken over all (i,j) in the domain of b. The domain of the erosion is the domain of f eroded by the domain of b.

In the edge detection problems that will approached in this paper, the domain of the structuring element will be chosen as the 4 - neighborhood of a pixel. Therefore, if this pixel is denoted by (0,0) the domain of the structuring element will be given by:

$$D = \{(0,-1), (0,1), (-1,0), (1,0) \}$$

Furthermore, only the case in which the value of the structuring element is null over this domain will be treated. Therefore, equations (3) and (4) reduce to:

$$d(r,c) = \max_{(i,j) \in D} (f(r-i,c-j)) \tag{5}$$

$$e(r,c) = \min_{(i,j) \in D} (f(r+i,c+j)) \tag{6}$$

3. EDGE DETECTION BY MATHEMATICAL MORPHOLOGY

Lee et al (2) proposed several edge detectors based on mathematical morphology theory. Among them, we may mention the following, which will be studied in this paper:

1) $G_e(r,c) = f(r,c) - e(r,c)$
2) $G_d(r,c) = d(r,c) - f(r,c)$
3) $G_{max}(r,c) = \max(G_e(r,c), G_d(r,c))$
4) $G_{min}(r,c) = \min(G_e(r,c), G_d(r,c))$

5) $G_{sum}(r,c) = G_e(r,c) + G_d(r,c)$
6) On define $G_{blur}(r,c) = G'_{min}(r,c)$ onde $G'_{min}(r,c)$ is detector 4) having as its input a blurred version of the original image f.

Lee et al (2) studied the performance of these detectors, including the behavior in the presence of noise, by concluding that, in general, the last of the previous detectors has the best performance.

4. EVALUATION OF THE PERFORMANCE OF MORPHOLOGICAL EDGE DETECTORS WITH RESPECT TO EDGE ORIENTATION

Abdou and Pratt (5) studied the performance of edge detectors based on enhancement and thresholding. This section presents the results of the application of one of the evaluation methods proposed by those authors (sensitivity with respect to edge orientation) in the case of morphological edge detectors.

The average intensities of different pixels of a 3x3 subregion containing the central edge are displayed in Figure 1. These intensities are given as functions of the orientation ϕ. Due to the symmetry of the detectors, it is enough to study the performance over the interval $0 < \phi < \pi/4$.
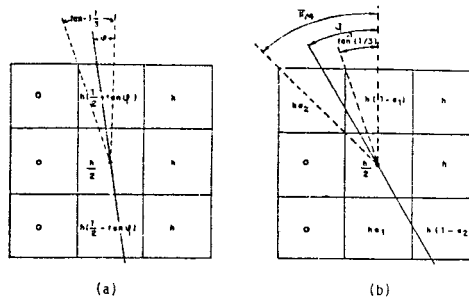
a - $0 < \phi < \arctan(1/3)$
b - $\arctan(1/3) < \phi < \pi/4$

Figure 1 - Edge models for orientation analysis - Source: (5)

Simple geometrical calculations can be performed to provide the output of the detectors as a function of the edge orientation for the chosen models. The result of these calculations refers to the interval $0 < \phi < \pi/4$, that was divided into two subintervals, $0 < \phi < \arctan$ (1/3) e $\arctan$ (1/3) $0 < \phi < \pi/4$, according to Figures 1(a) and 1(b), respectively.

The outputs of the basic operators (dilation and erosion) are computed as well as the outputs of the detectors G_e, G_d, G_{max} , G_{min} and G_{blur} over the interval $0 < \phi < \pi/4$. These results (normalized, i.e., divided by h where h is the maximum intensity of the pixel) are represented in Figure 2. One verifies that the outputs of the five detectors are independent of the edge orientation over the inverval $0 < \phi < \pi/4$.

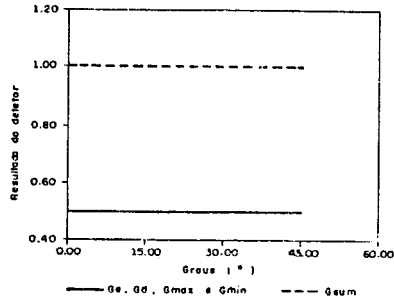Figure 2 - Normalized outputs of simple morphological edge
detector over the interval $0 < \phi < \pi/4$.

It should be emphasized that the outputs of the detectors are computed on
the central pixels of the 3x3 neighborhood.

In the case of the morphological edge detector G_{blur}, a blurring operation
is initially performed, which, in this paper, was implemented through the
average of the pixel values over a 3x3 neghborhood. Therefore, the output of the
detector depends on the values that are assumed by the pixels on the border of
the central neighborhood. Two situations were examined:

Case a) the pixels of the border have a constant value equal to $0 < \phi < \pi/4$.
Case b) the pixels of the border have values that are compatible with the
        continuation of the edge.

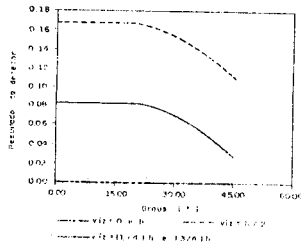The results obtained in case a) are displayed in Figure 3.

Figure 3 - Outputs of the G_{blur} detector over the interval $0 < \phi < \pi/4$
- constant ($= \alpha$) border pixels.

One observes that the detector output is null for $\alpha = 0$ and $\alpha = h$. For $\alpha =$
1/4 h and 3/4 h the output is constant and equal to h/12 up to $\phi = $ arctan 1/3
and from thereon the output is monotonically decreasing. The same behavior is
observed for $\alpha = h/2$, except the fact that the output value is the double of the
previous case (h/6).
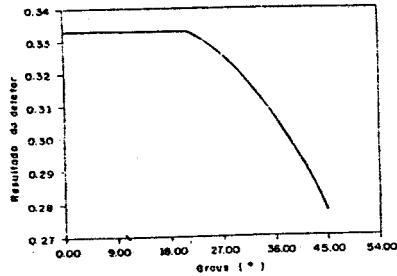
The results for case b) are displayed in Figure 4.

Figure 4 - Output of the G_{blur} detector over the interval $0 < \phi < \pi/4$
- border pixels according to continuation of edge.

One verifies that the detector has a constant output (equal to h/3) over the interval from 0 degrees up to approximately 26 degrees and presents a monotonically decreasing response from thereon.

5. EVALUATION OF THE PERFORMANCE ON MORPHOLOGICAL EDGE DETECTORS WITH RESPECT TO EDGE DISPLACEMENT

In this case the edge has a fixed orientation but the distance from the edge to the center of the detector is variable. The chosen orientations are vertical (horizontal displacement) and diagonal, with $\phi = 0$ and $\phi = \pi/4$, respectively, according to Figure 5.
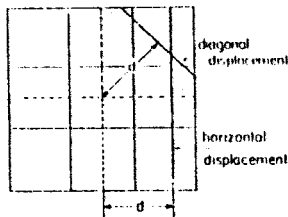

Figure 5 - Edge models for edge displacement sensitivity analysis - Source: (5)

5.1. HORIZONTAL DISPLACEMENT

Figures 6 (a), (b) and (c) display the sensitivity of the outputs of the morphological edge detectors G_d, G_{min}, G_e, G_{max} and G_{blur}. The results are combined in Figure 6 (d).
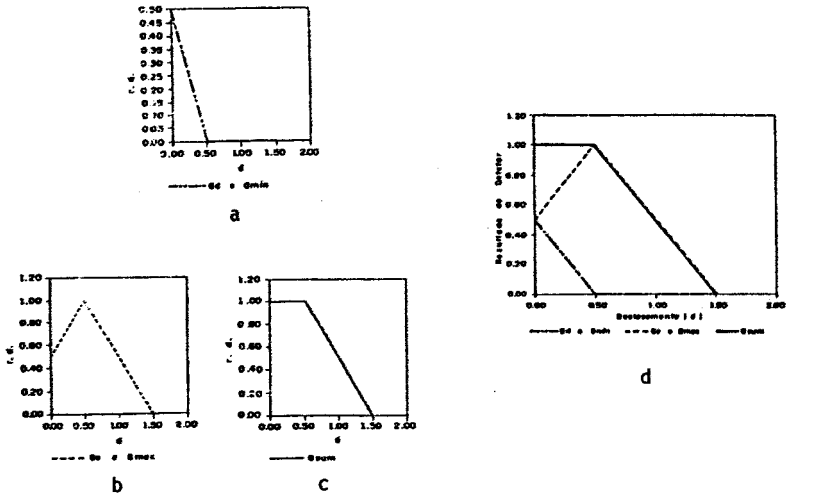
a

b

c

d

Figure 6 - Normalized outputs of simple morphological edge
detectors for horizontal displacement

One can observe that G_d, G_{min} and G_{sum} display a monotonically decreasing output with respect to horizontal displacement but this does not happen with G_e and G_{max}.

In the case of G_{blur}, similarly to the previous section, two types of borders were considered. In the case of constant value (equal to α), the performance is displayed in Figures 7 (a), (b), (c) and (d). The combined result is in Figure 7(e).
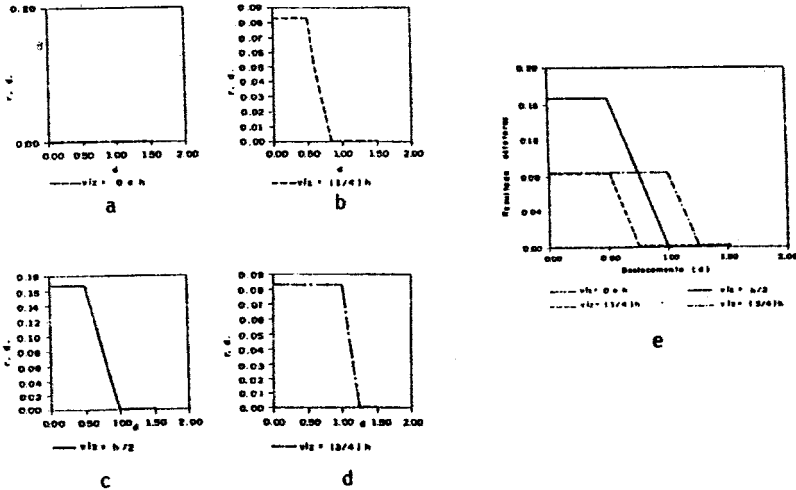

a

b

e

c

d

Figure 7 - Outputs of the G_{blur} detector for horizontal displacement
- constant ($=\alpha$) border pixels.
One verifies that the detector output is null for $\alpha = 0$ and $\alpha = h$ and monotonically decreasing after a certain threshold for other values of α.

The result for the case where the border values are selected as continuation of the edge is displayed in Figure 8.
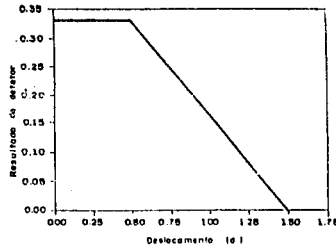

Figure 8 - Output of the G_{blur} detector for horizontal displacement
- border pixels according to continuation of edge

5.2. DIAGONAL DISPLACEMENT

Figures 9 (a), (b) and (c) display the sensitivity of the outputs of the morphological edge detectors G_d, G_{min}, G_e, G_{max} and G_{sum}. The results are combined in Figure 9 (d).
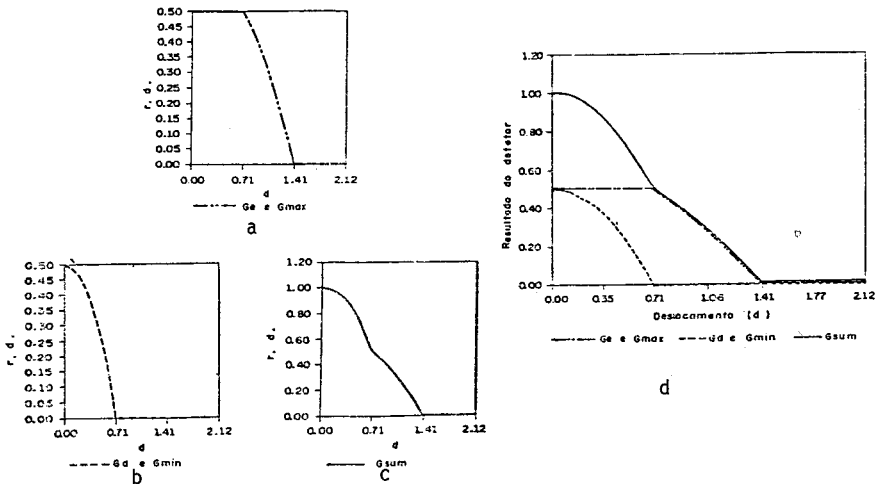

Figure 9 - Normalized outputs of simple morphological edge detectors
for diagonal displacement

One can observe that all five detectors display a monotonically decreasing output with respect to diagonal displacement.
As for G_{blur}, two types of border were considered. In the case of constant value (equal to α), the results are displayed in Figures 10 (a), (b), (c) and (d). The combined result is in Figure 10 (e).
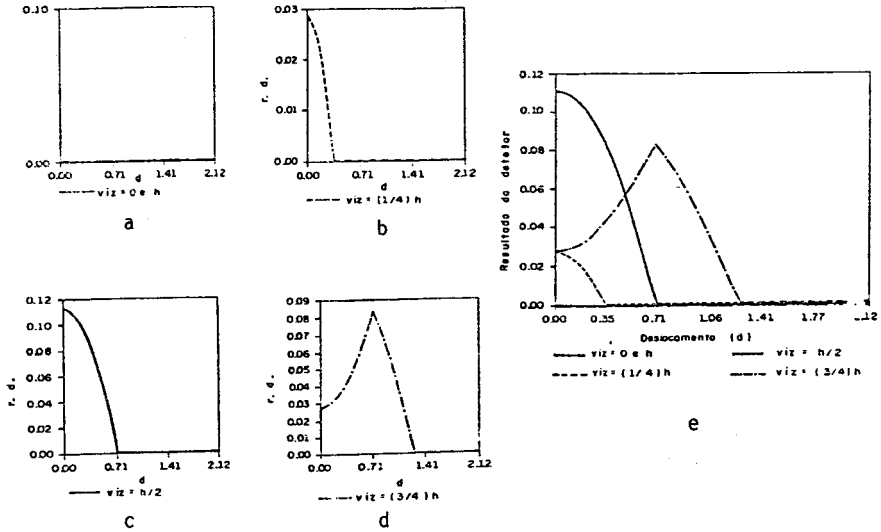
Figure 10 - Outputs of the G_{blur} detector for diagonal displacement
- constant (= α) border pixels.

The detector output is null for α = 0 and α = h, monotonically decreasing for α = 1/4 h and α = h/2 and has a peak value for d = $\frac{\sqrt{2}}{2}$ for α = 3/4 h.

The result for the case where the border values are selected as continuation of the edge is displayed in Figure 11.
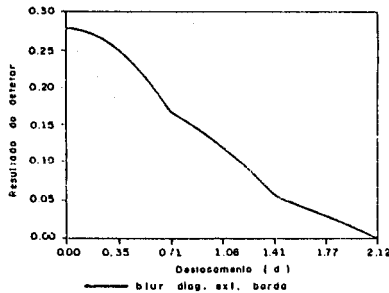

Figure 11 - Output of the G_{blur} detector for diagonal displacement
- border pixel according to continuation of edge

Observe that, in the case of horizontal displacement, the curves are either a constant or piecewise linear. On the other hand, with diagonal displacement the curves display quadratic behavior over some portions of the interval 0 <d< $\sqrt{2}$.

6. APPLICATION EXAMPLE

As an example of the application of a morphological edge detector (G_{blur}), a Landsat TM image, band 3, taken over the International Airport of Galeão, Rio de Janeiro, on August 8th, 1987, was used (Figure 12).
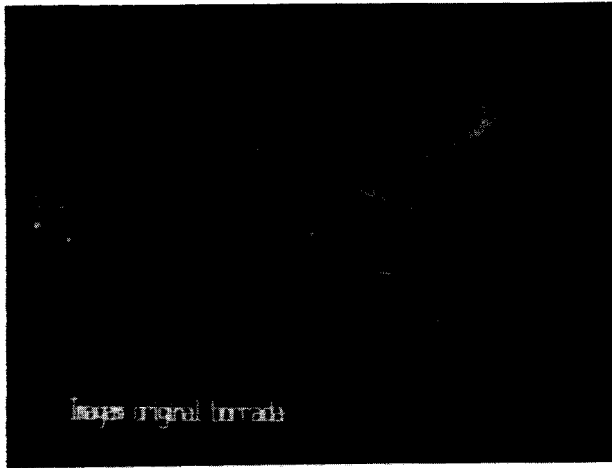
Figure 12 - Original Image

This image was blurred through a convolution mask of the type

$$\frac{1}{9} \quad \begin{array}{ccc} 1 & 1 & 1 \\ 1 & 1 & 1 \\ 1 & 1 & 1 \end{array}$$

The images that result from the operation of gray level erosion and dilation over the blurred image were obtained, according to equations (5) and (6), generating $G_e(r,c)$ and $G_d(r,c)$. A gray level image of $G_{blur}(r,c)$ was also obtained. The binary morphological edge detection image (Figure 13) was the result of the selection of a threshold above which 15% of the histogram of the gray level morphological edge detection image were obtained.

From the point of view of discrimination of closely spaced straight edges, the performance of the G_{blur} detector can be considered satisfactory. This can be observed from the separation of the largest and smallest runways of the airport that occur in the image.
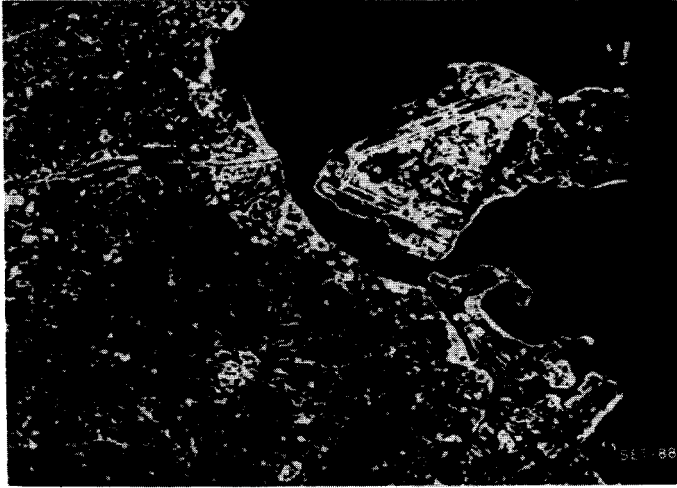
Figure 13 - Binary morphological edge image - G_{blur} operation

7 - CONCLUDING REMARKS

The desirable behavior for edge detectors with respect to edge orientation is an invariant response with this orientation. This type of performance was observed with the simple morphological detectors (not involving blur) ie , G_e, G_d, G_{max}, G_{min} and G_{sum}. On the other hand, the ideal behavior with respect to edge displacement (horizontal or diagonal) is a fast decrease with displacement. In this case, the best detectors were G_d and G_{min}(horizontal displacement) and G_{blur} (diagonal displacement for constant neighborhood equal to h/4). If one disregards the somewhat artificial situation of constant neighborhood, the best performance for diagonal displacement is given by G_d and G_{min}. A nonmonotonic decreasing response with displacement was observed with G_e and G_{max} (horizontal displacement) and G_{blur} (diagonal displacement with constant neighborhood equal to 3/4 h).

REFERENCES

(1) Jain, A.K. Fundamentals of digital image processing, Englewood Cliffs, N.J., Prentice Hall, 1989.

(2) Lee, J.S.; Haralick, R.M.; Shapiro, L.G. Morphologic edge detection. IEEE Journal of Robotics and Automation, RA-3(2): 142-156, April 1987.

(3) Matheron, G. Random sets and integral geometry, New York, N.Y., John Wiley, 1975.
(4) Serra, J. Image analysis and mathematical morphology, London, Academic Press, 1982.

(5) Abdou, I.E.; Pratt, W.K. Quantitative design and evaluation of enhancement/thresholding edge detectors. Proceedings of the IEEE, 65(5): 753-763, May 1979.